JACS
JOURNAL OF THE AMERICAN CHEMICAL SOCIETY
Communication
pubs.acs.org/JACS

Nucleation-Controlled Polymerization of Nanoparticles into Supramolecular Structures

Jing Wang,[†] Hongwei Xia,[§] Yanfeng Zhang,[‡] Hua Lu,[‡] Ranjan Kamat,[†] Andrey V. Dobrynin,[†] Jianjun Cheng,[‡] and Yao Lin*[,†,§]

[†]Polymer Program, Institute of Materials Science and [§]Department of Chemistry, University of Connecticut, Storrs, Connecticut 06269, United States

[‡]Department of Materials Science and Engineering, University of Illinois at Urbana−Champaign, Urbana, Illinois 61801, United States

Supporting Information

ABSTRACT: Controlled assembly of inorganic nanoparticles (NPs) into structurally defined supramolecular polymers will create nanomaterials with new collective properties. However, supramolecular polymerization of isotropic NPs remains a challenge because of the lack of anisotropic interactions in these monomers to undergo directional associations for the cooperative growth of supramolecular chains. Herein we report self-assembly behavior of poly(L-glutamic acid)-grafted gold NPs in solution and describe how combined attractive and repulsive interactions influence the shape and size of the resulting supramolecular assemblies. The study shows that the chain growth of supramolecular polymers can be achieved from the NP monomers and the process occurs in two distinct stages, with a slow nucleation step followed by a faster chain propagation step. The resulting supramolecular structures depend on both the grafting density of the poly(L-glutamic acid) on the NPs and the size of the NPs.

Ensembles of inorganic nanoparticles (NPs) may possess collective properties that are superior to those of individual NPs and bulk samples.[1] Technological applications of NPs rely on the ability to control the cooperative interactions of NPs in the ensembles in order to exploit their ordered structures and collective properties.[2] Much progress has been made in the self-assembly and directed assembly of NPs into different types of nanostructures with unique optical, electronic, and magnetic properties.[3] However, success has been limited in the prediction and control of the architecture of NP assemblies and the kinetic process of assembly.[4]

In remarked contrast, globular proteins can be "polymerized" into specific helical or tubular assemblies via a well-defined nucleation−growth mechanism (i.e., cooperative supramolecular polymerization), as exemplified by the formation of actin filaments, microtubules, and bacteria flagella.[5] In these biological processes, the association of several protein monomeric units first forms an aggregate that serves as the nucleation center and template for the docking of additional protein monomers, resulting in a chain propagation of protein polymers. The unique disposition of the repeating units in filamentous structures and the multiple coordinated interactions between the units give rise to the molecular cooperativity required for the fast chain growth into large supramolecular structures.[5] Inspired by the sophisticated assembly mechanisms in the biological processes, we developed a strategy to rationally design NP building blocks that undergo cooperative supramolecular polymerization into NP assemblies (Scheme 1).

Scheme 1. Nucleation-Controlled Assembly of Polypeptide-Grafted Nanoparticles into Fibrous or Globular Supramolecular Structures

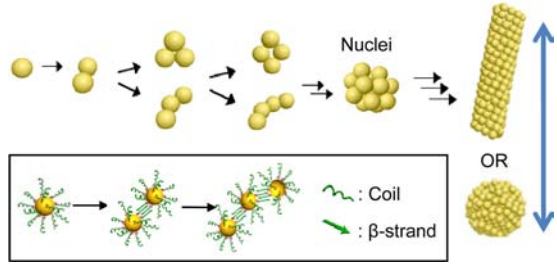

We find three basic design requirements must be met in order to facilitate controlled supramolecular polymerization of NP monomers. First, the monomers should have multiple sites that allow specific and coordinated noncovalent interactions ("bonding"). This requirement can be met by the synthesis of NPs covered with ligands that are subject to multivalent H-bonding for cohesive interactions. Synthetic polypeptides, such as poly(L-glutamic acids) (PLGs), are well-known for their intermolecular H-bonding and therefore are excellent candidates for this purpose.[6]

Second, the monomers need to adopt a relatively high-energy state to allow for thermodynamically favored incorporation of NPs into the supramolecular structure. This requirement can be met by controlling the reaction conditions to tune the conformation of the surface ligands to different stabilities. PLGs can respond to environmental changes by adopting different secondary structures.[7] At appropriate pH and temperature, the grafted PLGs can have partially extended coil structures in solutions, as some side-chain carboxylate groups

Received: March 18, 2013
Published: May 22, 2013

   dx.doi.org/10.1021/ja402757e | J. Am. Chem. Soc. 2013, 135, 11417−11420

are deprotonated. Upon the assembly of NPs grafted with PLGs (NP-*g*-PLG) into superstructures with intermolecular PLG-chain intercalation, the conformation of grafted PLGs can evolve to the more thermodynamically stable β-sheet structure (Scheme 1).[6b]

Third, for spherical NPs that do not possess the inherent anisotropy to undergo directional interactions in a well-defined helical/tubular polymerization mechanism, specific repulsive forces between monomers need to be present in order to make fibrous supramolecular structure.[4d,8] Without a preventive force, globular aggregates of NPs would be thermodynamically most favorable. In the case of NP-*g*-PLG, the repulsive forces can come from the electrostatic interactions between the partially charged PLGs on NP surface. The third requirement is less obvious than the previous two but can play a central role in control of NP assembly architectures.

We first consider how the electrostatic interactions and association energies influence the shape and size of charged NP aggregates. Formation of multiparticle aggregates is driven by the difference in the NP chemical potentials between aggregated and dispersed states. The aggregates begin to form when the NP concentration exceeds a critical aggregation concentration (X_{crit}).[8b] To describe formation of globular and fibrous aggregates consisting of N particles,[9] we approximate the shape of a NP aggregate by an ellipsoid with an axial ratio p ($p = 1$ for spheres, $p < 1$ for prolate spheroids, and $p \ll 1$ for rods). The change in standard chemical potential of the charged NP in an aggregate has contributions from the particle−particle "bond" energy in the assembly relative to isolated particles in solution, the increase of energy from unsaturated "bonds" from the particles on the surface of the aggregate and electrostatic repulsion between charged groups. In this approximation, the standard chemical potential can be expressed as

$$\Delta\mu_N^0(N, p) = k_BT\left[-n\varepsilon + \frac{(n - n')\varepsilon}{N^{1/3}}g(p) + \frac{N^{2/3}l_Bz^2f(p)}{d}\right] \quad (1)$$

where n and n' are the number of nearest neighbors per particle in the bulk and on the surface, respectively; ε is the "bond" energy between two neighboring particles in terms of the thermal energy k_BT; l_B is the Bjerrum length determining strength of the electrostatic interactions; d is the center-to-center distance between neighboring particles; z is the number of charges per particle; $g(p)$ and $f(p)$ are geometric functions of the shape factor p (see Supporting Information, SI).

The most probable size (N) and shape (p) of the NP assemblies are determined by finding the minimum of the chemical potential in eq 1. Our study shows that there are two local minima corresponding to $p = 1$ with finite N and $p \ll 1$ with a very large N (Figure 1). The stability of particular aggregate is governed by the value of the dimensionless parameter $\delta = l_Bz^2/d(n - n')\varepsilon$. Increasing the value of the parameter δ favors the formation of globule aggregates ($p = 1$) with a finite N. Long fibrous aggregates may be found in the systems with sufficiently small values of δ. The value of δ is varied by changing the grafting densities of PLGs on NPs (causing z and ε to change proportionally). Based on this model, we synthesized NP-*g*-PLG with different grafting densities and investigated the supramolecular assemblies from these particles and the kinetics of the assembly process.

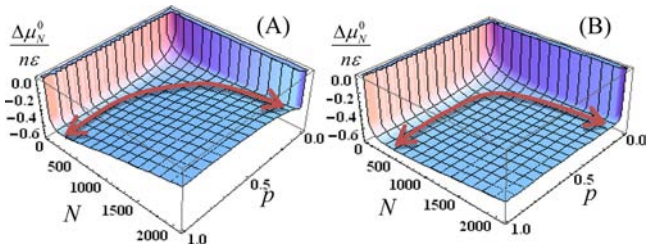

Figure 1. The relative energetic stability of globular and fibrous aggregates at the δ equal to (A) 0.015 and (B) 0.006.

NP40-*g*-PLG$_{55}$, with an average core diameter of 40 nm for gold NPs and a degree of polymerization (DP) of 55 for PLG grafted on the surface, was synthesized and characterized using our previously reported method (Schemes S1−2).[6b] Unbound PLG-SH (PLGs end-functionalized with thiols) was removed from the solution after the synthesis of NP-*g*-PLG, and the PLG grafting densities on NPs were quantified by ^{1}H NMR spectroscopy (Figures S1−2). The ligand coverage was found to be tunable by controlling the initial amount of PLG-SH added into the synthesis of NP-*g*-PLG and the incubation condition. Three NP40-*g*-PLG$_{55}$ samples, denoted as NP40-*g*-PLG$_{55}$-I, -II and -III, were made by the above procedure and the average numbers of ligands bounded on each particle were determined to be around 2×10^3, 9×10^2, and 2×10^2, respectively (Figure S2).

NP40-*g*-PLG$_{55}$ samples with different grafting densities were incubated in water with the pH adjusted to 6.5 (added salt concentration <5 mM) and 4 °C. Under these selected conditions, NP-*g*-PLG has partially charged PLG side chains, allowing the NP-*g*-PLG to be water-soluble and also have reduced charge repulsion to facilitate the interparticle PLG-chain intercalation and subsequent formation of β-sheet conformation for stable supramolecular structures (see Scheme 1).[6b] All NP40-*g*-PLG$_{55}$ samples were well-dispersed in their monomeric form initially, but they started to form supramolecular structures after a few days. The supramolecular structures evolved in solution were examined by TEM after incubation for 1, 3, 7, 20 days (Figure 2D−F). As predicted, for the particles with a high grafting density of PLGs on the surfaces (NP40-*g*-PLG$_{55}$-I with a largest δ in the three samples, Figure 2D), the resulting supramolecular structures were globular. The particles with the medium grafting density of PLGs (NP40-*g*-PLG$_{55}$-II, Figure 2E) assembled into short fibrous structure. Long fibrous structures were only assembled from particles with a low PLG grafting density (NP40-*g*-PLG$_{55}$-III, Figure 2F).

The kinetic process of the supramolecular polymerization was studied by monitoring the concentration change of NP-*g*-PLG in pH 6.5 solutions over time using absorption spectroscopy (Figure 2A−C). For each sample, five solutions with different concentrations were first filtered to remove dust and other impurities in order to avoid nucleation on a foreign substrate, after which they were incubated at 4 °C. The formation of supramolecular structures depleted the freely dispersed NP-g-PLG in solution, corresponding to the decrease in the absorption of the supernatants. Figure 2A−C shows that, above a critical particle concentration, the growth of the supramolecular structures for all three samples occurred in two distinct stages, with a slow nucleation step followed by fast propagation. A sigmoidal transition was always found in these kinetic experiments (see the fitting in Figure 2A−C), indicating a cooperative process in the supramolecular polymerizations.

dx.doi.org/10.1021/ja402757e | J. Am. Chem. Soc. 2013, 135, 11417−11420

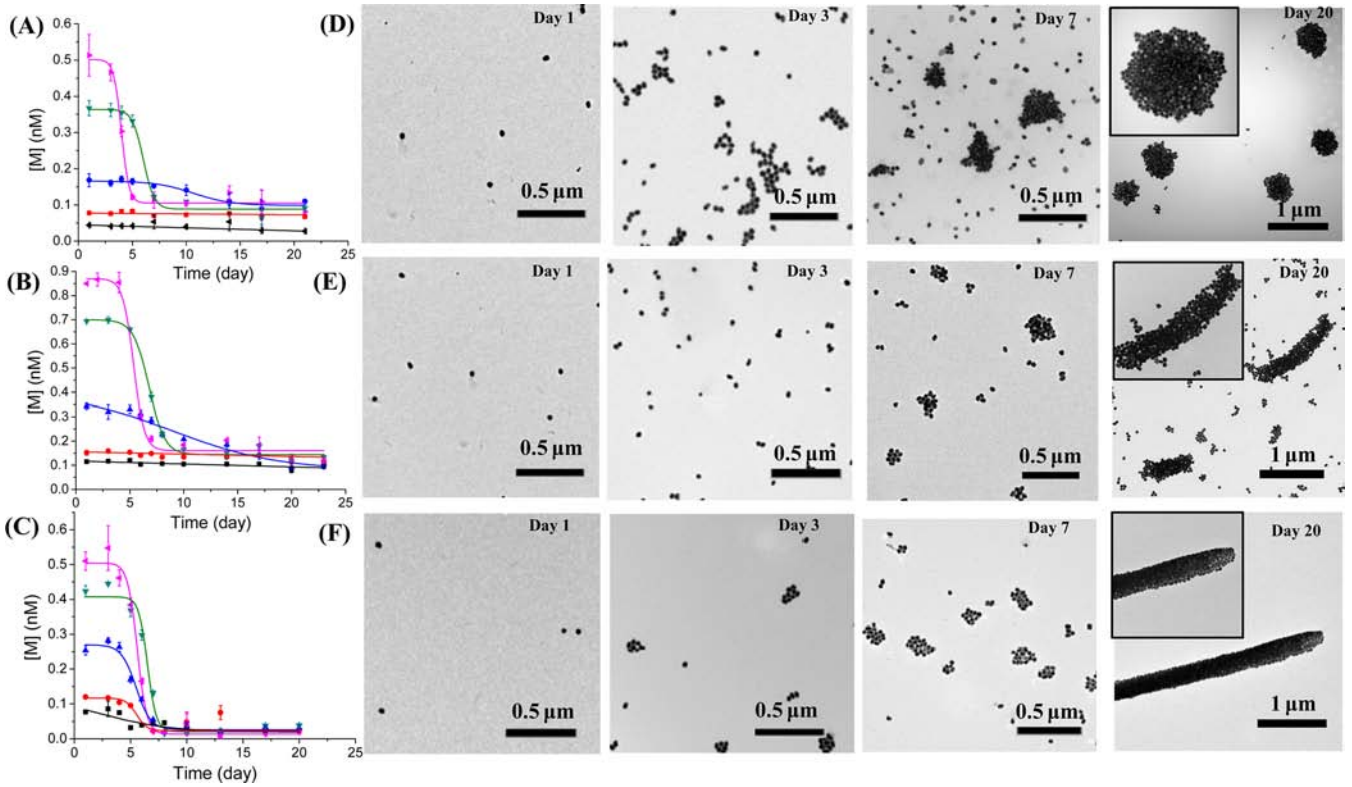

Figure 2. Type of supramolecular structures and kinetics of their formation depend on the grafting densities of PLGs on NPs. (A–C) Supramolecular polymerization kinetics of NP40-*g*-PLG_{55}-I, -II, and -III with PLG coverage of 100%, 40%, and 10%, respectively, at pH 6.5 and 4 °C. Five different initial concentrations were used for each NP40-*g*-PLG_{55}. (D–F) TEM images of the NP40-*g*-PLG_{55}-I, -II, and -III and their supramolecular structures in solution after incubation for 1, 3, 7, and 20 days. The initial particle concentration is 0.17, 0.34 and 0.24 nM, respectively.

From the kinetic experiments shown in Figure 2, the critical aggregation concentrations (X_{crit}) for NP40-*g*-PLG_{55}-I, II, and III at pH 6.5 and 4 °C were derived to be $1.8(\pm0.2) \times 10^{-12}$, $2.5(\pm0.4) \times 10^{-12}$, and $4.0(\pm0.4) \times 10^{-13}$, in the unit of mole fraction. As $X_{crit} \approx e^{\Delta\mu_N^0/k_BT}$,[8b] the change of standard chemical potential of NP40-*g*-PLG_{55} in the assembly relative to isolated particles was found to be in the scale of −27.1, −26.7, and $-28.6k_BT$ for the three samples. These free energy changes provide thermodynamic driving forces for the formation of stable supramolecular structures. The most stable structure was found in the fibrous supramolecular polymers assembled from NP40-*g*-PLG_{55}-III.

We then closely examined the nucleation-controlled polymerization of NP40-*g*-PLG_{55}-III that resulted in a fibrous supramolecular structure. Although a nucleation event, such as the closure of a ring, a tube, or the completion of the first turn of a helix, is often visualized as a singular steric step, we did not observe these special structures in the early stage of the oligomerization (Figure 2F). From a thermodynamic point of view, nucleation does not require such special structures as the turning point in stability for the chain growth. The formation of different clusters (see Scheme 1) may illustrate a more realistic nucleation process for NP-*g*-PLG, based on the experimental observations. The time course of the supramolecular polymerization (Figure 2C) shows that the concentration of polymerized particles increases much more abruptly than the t^2 dependence predicted in the classic theory by Oosawa,[5c] that described the homogeneous nucleation and growth of protein polymers. The autocatalysis observed in our experiments strongly suggests the existence of a secondary mechanism[10] for poly(NPs) formation (e.g., heterogeneous nucleation on the surface of poly(NPs) once they are formed). Detailed investigations focusing on the early stage of supramolecular polymerization using light scattering or other in situ methods will provide further insight into the exact secondary pathway of the nucleation process in the system.

Poly(NP40-*g*-PLG_{55}), the equilibrium supramolecular structure assembled from NP40-*g*-PLG_{55}-III, was isolated and examined by electron microscopy and found to form long, fibrous structures (Figure S3A). Poly(NP40-*g*-PLG_{55}) appeared to be shorter and more rigid than the tubular supramolecular structures assembled from PLG-grafted comb polymers in our previous study.[6b] The formation of β-sheet structures between PLG grafts was confirmed via staining of poly(NP40-*g*-PLG_{55}) with thioflavin T dye (ThT) (Figure S3B), a fluorescent molecule that is known for its strong, specific affinity to β-sheet structures.[11] The nature of the β-sheet structure was further revealed by FTIR analysis (Figure S4). The structural change of the grafted PLGs on the NPs during the assembly process allows for thermodynamically favored growth of supramolecular structure. The extinction spectra of NP40-*g*-PLG_{55} in solution recorded before and after the formation of supramolecular structures are given in Figure S5 and show the emergence of red-shifted plasmon resonance due to interparticle coupling.

Encouraged by the qualitative agreement between the thermodynamics analysis and the experimental data for NP40-*g*-PLG_{55}, we next prepared NP20-*g*-PLG_{55} with a core size of 20 nm and DP of 55 for PLG to test the general applicability of the assembly mechanism. Figure 3A shows that globular assemblies with finite size were obtained as the equilibrium structure for particles with a high grafting density of PLG (~400 ligands per

dx.doi.org/10.1021/ja402757e | J. Am. Chem. Soc. 2013, 135, 11417–11420

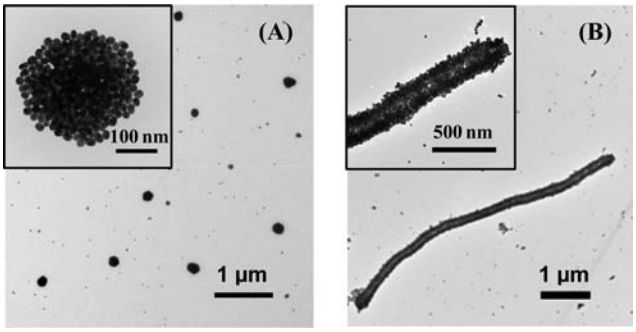

Figure 3. TEM images of supramolecular structures assembled from NP20-*g*-PLG$_{55}$ with (A) high and (B) low grafting densities, in solution at pH 6.5 and 4 °C.

particle). Interestingly, filamentous poly(NP20-*g*-PLG$_{55}$) assembled from NP20-*g*-PLG$_{55}$ with low PLG grafting density (~100 ligands per particle) showed distinct character as multiwall hollow tubes (Figure 3B). Plasmon resonance was also found in the these poly(NP20-*g*-PLG$_{55}$) structures (Figure S6). The geometry of a hollow tubule was not included in eq 1, which is based on a generalized ellipsoid shape function. Although a similar free energy analysis can be carried out for a given shape, a prediction of phase transitions requires the explicit evaluation of the prefactor for each energy term in the equation. Elucidating the complete phase diagram for the supramolecular assembly of NP-*g*-PLG is the subject of future study and requires high-resolution structural information on the orientation and distribution of grafted PLGs on NP surface, the consideration of the counterions, the suppression of charge dissociations in PLGs during assembly, and the distortion of the electric field at the boundaries.

In conclusion, we demonstrated supramolecular polymerization of polypeptide-grafted NPs by controlling their interactions under specific environmental conditions. The resulting supramolecular structures are strongly correlated to the grafting density of the polypeptides on the NPs and the sizes of the NPs. Thermodynamic analysis indicated the delicate role of the electrostatic interactions between the charged NPs in the assembly process. The controlled supramolecular polymerization process allows us to access fibrous poly(NPs) as new materials with potentially interesting collective properties. This approach should be applicable for a variety of NPs and their hybrids that are amenable to surface modification with polypeptides. If precise controls over the interparticle spacing and the mechanical strength can be realized in the supramolecular structures, these poly(NPs) may find potential applications in plasmonics and optoelectronics.

■ ASSOCIATED CONTENT

Supporting Information

Material synthesis, experimental procedures, and characterization data. This information is available free of charge via the Internet at http://pubs.acs.org.

■ AUTHOR INFORMATION

Corresponding Author

ylin@ims.uconn.edu

Notes

The authors declare no competing financial interest.

■ ACKNOWLEDGMENTS

This work was supported by the National Science Foundation (DMR-1150742). J.C. acknowledges support from NIH (1R21EB013379) and NSF (CHE-1153122). A.V.D. acknowledges support from NSF (DMR-1004576). We thank Dr. Carol Norris at the UConn Confocal Microscopy Facility for training, advice, and use of instrumentation, Virge Kask at UConn Biology Central Services for scientific illustration, and Prof. Douglas Adamson for helpful inputs to the manuscript.

■ REFERENCES

(1) (a) Luk'yanchuk, B.; Zheludev, N. I.; Maier, S. A.; Halas, N. J.; Nordlander, P.; Giessen, H.; Chong, C. T. *Nat. Mater.* **2010**, *9*, 707–715. (b) Nie, Z. H.; Petukhova, A.; Kumacheva, E. *Nat. Nanotechnol.* **2010**, *5*, 15–25. (c) Rycenga, M.; Cobley, C. M.; Zeng, J.; Li, W. Y.; Moran, C. H.; Zhang, Q.; Qin, D.; Xia, Y. N. *Chem. Rev.* **2011**, *111*, 3669–3712. (d) Talapin, D. V.; Lee, J. S.; Kovalenko, M. V.; Shevchenko, E. V. *Chem. Rev.* **2010**, *110*, 389–458. (e) Fan, J. A.; Wu, C. H.; Bao, K.; Bao, J. M.; Bardhan, R.; Halas, N. J.; Manoharan, V. N.; Nordlander, P.; Shvets, G.; Capasso, F. *Science* **2010**, *328*, 1135–1138. (f) Klajn, R.; Bishop, K. J. M.; Fialkowski, M.; Paszewski, M.; Campbell, C. J.; Gray, T. P.; Grzybowski, B. A. *Science* **2007**, *316*, 261–264.

(2) (a) Ghosh, S. K.; Pal, T. *Chem. Rev.* **2007**, *107*, 4797–4862. (b) Elghanian, R.; Storhoff, J. J.; Mucic, R. C.; Letsinger, R. L.; Mirkin, C. A. *Science* **1997**, *277*, 1078–1081. (c) Liu, N.; Hentschel, M.; Weiss, T.; Alivisatos, A. P.; Giessen, H. *Science* **2011**, *332*, 1407–1410.

(3) (a) Shenhar, R.; Norsten, T. B.; Rotello, V. M. *Adv. Mater.* **2005**, *17*, 657–669. (b) Srivastava, S.; Kotov, N. A. *Soft Matter* **2009**, *5*, 1146–1156. (c) Sun, S. H.; Murray, C. B.; Weller, D.; Folks, L.; Moser, A. *Science* **2000**, *287*, 1989–1992. (d) Tang, Z. Y.; Kotov, N. A. *Adv. Mater.* **2005**, *17*, 951–962. (e) Akcora, P.; Liu, H.; Kumar, S. K.; Moll, J.; Li, Y.; Benicewicz, B. C.; Schadler, L. S.; Acehan, D.; Panagiotopoulos, A. Z.; Pryamitsyn, V.; Ganesan, V.; Ilavsky, J.; Thiyagarajan, P.; Colby, R. H.; Douglas, J. F. *Nat. Mater.* **2009**, *8*, 354–359. (f) Nykypanchuk, D.; Maye, M. M.; van der Lelie, D.; Gang, O. *Nature* **2008**, *451*, 549–552. (g) Sharma, J.; Chhabra, R.; Cheng, A.; Brownell, J.; Liu, Y.; Yan, H. *Science* **2009**, *323*, 112–116.

(4) (a) Liu, K.; Nie, Z. H.; Zhao, N. N.; Li, W.; Rubinstein, M.; Kumacheva, E. *Science* **2010**, *329*, 197–200. (b) Macfarlane, R. J.; Lee, B.; Jones, M. R.; Harris, N.; Schatz, G. C.; Mirkin, C. A. *Science* **2011**, *334*, 204–208. (c) Ribeiro, C.; Lee, E. J. H.; Longo, E.; Leite, E. R. *ChemPhysChem* **2006**, *7*, 664–670. (d) Groenewold, J.; Kegel, W. K. *J. Phys. Chem. B* **2001**, *105*, 11702–11709.

(5) (a) Oosawa, F.; Asakura, S. *Thermodynamics of the Polymerization of Protein*; Academic Press: London, U.K., 1975. (b) De Greef, T. F. A.; Smulders, M. M. J.; Wolffs, M.; Schenning, A.; Sijbesma, R. P.; Meijer, E. W. *Chem. Rev.* **2009**, *109*, 5687–5754. (c) Oosawa, F.; Kasai, M. *J. Mol. Biol.* **1962**, *4*, 10–21. (d) Zhao, D. H.; Moore, J. S. *Org. Biomol. Chem.* **2003**, *1*, 3471–3491.

(6) (a) Mondeshki, M.; Mihov, G.; Graf, R.; Spiess, H. W.; Mullen, K.; Papadopoulos, P.; Gitsas, A.; Floudas, G. *Macromolecules* **2006**, *39*, 9605–9613. (b) Wang, J.; Lu, H.; Kamat, R.; Pingali, S. V.; Urban, V. S.; Cheng, J. J.; Lin, Y. *J. Am. Chem. Soc.* **2011**, *133*, 12906–12909.

(7) (a) Nagasawa, M.; Holtzer, A. *J. Am. Chem. Soc.* **1964**, *86*, 538–543. (b) Oneil, K. T.; Degrado, W. F. *Science* **1990**, *250*, 646–651. (c) Spek, E. J.; Gong, Y. X.; Kallenbach, N. R. *J. Am. Chem. Soc.* **1995**, *117*, 10773–10774. (d) Krimm, S. *Biopolymers* **1972**, *11*, 2309–2316.

(8) (a) Min, Y. J.; Akbulut, M.; Kristiansen, K.; Golan, Y.; Israelachvili, J. *Nat. Mater.* **2008**, *7*, 527–538. (b) Israelachivili, J. *Intermolecular and Surface Forces*, 3rd ed.; Academic Press: Waltham, MA, 2011.

(9) Oosawa, F. *J. Polym. Sci.* **1957**, *26*, 29–45.

(10) (a) Bishop, M. F.; Ferrone, F. A. *Biophys. J.* **1984**, *46*, 631–644. (b) Ferrone, F. *Methods Enzymol.* **1999**, *309*, 256–274. (c) Ferrone, F. A.; Hofrichter, J.; Eaton, W. A. *J. Mol. Biol.* **1985**, *183*, 611–631.

(11) (a) Levine, H. *Protein Sci.* **1993**, *2*, 404–410. (b) LeVine, H. *Methods Enzymol.* **1999**, *309*, 274–284.